Antarct. Meteorite Res., **18**, 83–95, 2005

Visible and near-infrared reflectance spectroscopy of the Yamato 980459 meteorite in comparison with some shergottites

Takahiro Hiroi[1]*, Masamichi Miyamoto[2], Takashi Mikouchi[2] and Yuji Ueda[2]

[1]*Department of Geological Sciences, Brown University, Providence, RI 02912, U.S.A.*
[2]*Department of Earth and Planetary Science, University of Tokyo, Hongo 7-chome, Bunkyo-ku, Tokyo 113–0033*
**Corresponding author. E-mail: takahiro_hiroi@brown.edu*

(Received November 17, 2004; Accepted January 24, 2005)

Abstract: Visible and near-infrared reflectance spectrum of a sample of Yamato (Y) 980459 meteorite has been measured. Preliminary analyses of the spectrum have been performed using the modified Gaussian model, and the results have been compared with those of similar analyses of some shergottites and tricomponent mixtures of olivine, pyroxene, and plagioclase. They suggest that Y980459 has lower Fe and/or Ca concentration in pyroxene phase except its high-Ca pyroxene having similar Fe/Ca concentration to EETA79001 (Lithology A), lower pyroxene abundance, and more glassy phase than those shergottite samples. An estimated pyroxene modal abundance of this Y980459 sample is 36±13%, which is consistent with another estimate of 48% by an independent petrographic study.

key words: Yamato 980459, shergottite, reflectance spectrum, modified Gaussian model, deconvolution

1. Introduction

A relatively new meteorite, Yamato (Y) 980459, is a unique member of martian meteorites, being similar to olivine-phyric shergottites but different from previously known members in several respects (*e.g.*, Kojima and Imae, 2002; Mikouchi *et al.*, 2003; Greshake *et al.*, 2003; Ikeda, 2003). In view of the importance of reflectance spectroscopy as a tool for non-destructive analysis of mineralogy and remote sensing of Mars, we have conducted a measurement of this meteorite sample and compared the result with those of several shergottite samples and mixtures of common geologic minerals, mainly utilizing the modified Gaussian model (Sunshine *et al.*, 1990) to deconvolve the measured spectra into individual absorption bands. Information expected to be gained through reflectance spectroscopy of this sample is mainly its mineral modal abundance and Fe and/or Ca contents of its pyroxenes. This study was conducted as a part of the Y980459 consortium study (Misawa, 2003).

2. Experimental

Fresh samples of Y980459 were supplied by National Institute of Polar Research. Two chips of 106 mg in total were ground in a corundum mortar and sieved to obtain a $<100\,\mu$m powder sample. The sample was placed in a 1.5-mm deep sample holder. Biconical diffuse reflectance spectra were measured using a UV-Visible-Near IR spectrophotometer with the incident angle of 30 degrees and emission angle of 0 degree. Two detectors, a photomultiplier in the range of 200–820 nm and a PbS cell cooled at 0°C in the range of 820–2500 nm were used. The light sources were a deuterium lamp in the spectral range of 200–300 nm and a tungsten lamp in the range of 300–2500 nm. The spectra were scanned at a constant rate of 1 nm/s and were recorded every 2 nm using Halon as a reflectance standard. The measured reflectance spectra were corrected for the absolute reflectance of Halon based on an NBS table. Dry air was pumped into the spectrometer chamber throughout the spectral measurements for suppressing absorption by water in the air.

Similarly-measured bidirectional reflectance spectra of powder samples of shergottite: Shergotty, Zagami, EETA79001 (McFadden and Cline, 2004) and tricomponent mixtures of olivine, orthopyroxene, and plagioclase powders (Hiroi and Pieters, 1994) were taken from the RELAB database (Pieters, 1983; http://lf314-rlds.geo.brown.edu/) for comparison.

The modified Gaussian model deconvolution (Sunshine *et al*., 1990) was performed for each of the above reflectance spectra. The optimization of parameters was performed by initially starting with a continuum background which contacts with each spectrum (natural logarithm of reflectance over the wavelength range of 0.5 to 2.5 μm) at both sides of the 1-μm band (around 0.55 or 0.7 μm and around 1.4 μm) and the minimum number of modified Gaussians centering at around 0.45, 0.65, 0.95, 1.2, and 1.9 μm. After the initial optimization, the number of modified Gaussians is increased until the residual error becomes reasonably small (being at the comparable level of the measurement errors and having no systematic trend). Then, another optimization calculation was made starting with the final solution parameter values with the relative strengths between the bands 1a and 1b and between the bands 2a and 2b changed. If it led to a different solution with a similar error level to the first solution, it was also adopted as another solution. Solutions with a negative inclination of the continuum background or having two modified Gaussians with very close center wavelengths were rejected.

3. Results and discussion

Shown in Fig. 1 are the reflectance spectrum of the Y980459 sample measured in this study (solid line) and reflectance spectra of some shergottites (broken lines): EETA 79001 lithologies A and B, Shergotty, and Zagami (Sunshine *et al*., 1993; McFadden and Cline, 2004) taken from the RELAB database. It is clear that Y980459 has a totally different reflectance spectrum from any of these shergottites in that it is darker, its absorption bands are shallower, and especially its 2-μm band strength relative to its 1-μm band strength is much smaller than those of these shergottites. The Y980459

spectrum also lacks the two sharp bands near 0.5 μm which are common to all these shergottites.

In order to elucidate the characteristics of the Y980459 spectrum, the modified Gaussian model deconvolution (Sunshine *et al*., 1990) has been applied to it. The result is shown in Fig. 2, and the optimized continuum background and modified

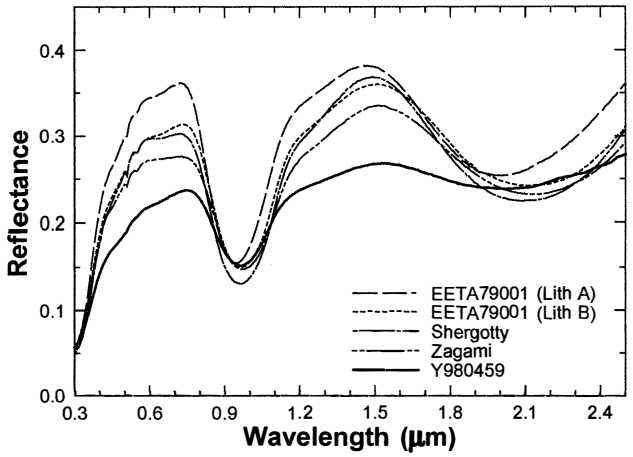

Fig. 1. Reflectance spectrum of a powder sample of Y980459 measured in this study and reflectance spectra of some shergottite powder samples (Sunshine et al., 1993; McFadden and Cline, 2004) taken from the RELAB database.

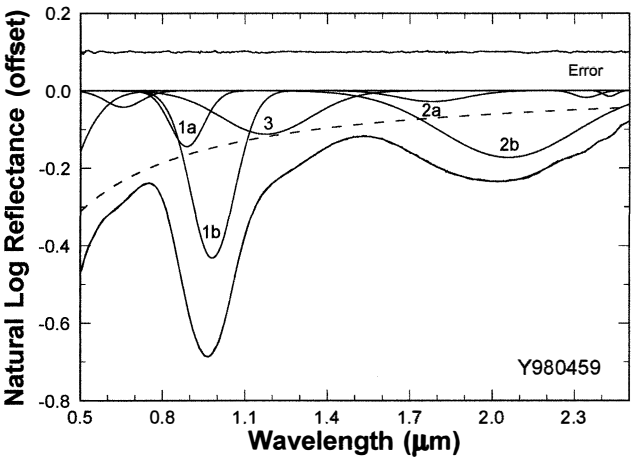

Fig. 2. Modified Gaussian model deconvolution of the reflectance spectrum of the Y980459 sample. Shown in a broken line is the continuum background spectrum, and shown in a solid line above 0 of the vertical axis is the residual error spectrum. The measured, fitted, and continuum background spectra are shifted by a common offset, and the residual error spectrum by +0.1. Band numbers are assigned to modified Gaussians representing the major absorption bands discussed in this paper.

Table 1. Optimized parameters and root mean square deviation (RMSD) for a modified Gaussian model fit of the reflectance spectrum of Y980459.

	c_0	c_1 (μm)	RMSD
	−1.177	−0.167	0.00131
Band No.	Center (μm)	FWHM (μm)	Strength
	0.289	0.315	−0.545
	0.656	0.154	−0.042
1a	0.888	0.144	−0.144
1b	0.982	0.189	−0.432
3	1.176	0.383	−0.112
2a	1.780	0.292	−0.028
2b	2.058	0.583	−0.172
	2.343	0.103	−0.018
	2.428	0.055	−0.015

Gaussian parameters are listed in Table 1. There are two sets of major bands around 1 and 2 μm due to Fe^{2+} in the M2 site of Ca-poor (bands 1a and 2a) and Ca-rich (bands 1b and 2b) pyroxene, a shoulder band near 1.2 μm (band 3) due to either Fe^{2+} in plagioclase, olivine, or pyroxene (M1 site), some short-wavelength bands, and two minor bands around 2.3–2.4 μm probably due to weathering. Because olivine should have two other absorption bands beside the band 3, the bands 1a and 1b should contain those olivine bands in a complex way, which this version of the modified Gaussian model algorithm is unable to resolve. Existence of other minerals such as glass would also make it difficult to assign the deconvolved bands near 1 μm to the individual components. Y980459 does have a mesostasis phase by as much as 25% (Mikouchi *et al.*, 2004). Analysis and discussion in this study will not be carried beyond this limitation.

The same deconvolution procedure has been performed to each of the reflectance spectra of shergottite samples shown in Fig. 1. The results are shown in Fig. 3 and listed in Table 2. There are two similarly good devonvolution solutions for Shergotty (Figs. 3a and 3b) and Zagami (Figs. 3c and 3d) which have different initial parameter values. EETA79001 lithology A (Fig. 3e) and B (Fig. 3f) had only one good solution, respectively. These results with Shergotty and Zagami samples suggest that the relative strength between low-Ca and high-Ca pyroxenes in these samples cannot be reliably estimated from this method. A more realistic interpretation is that the Ca content of pyroxenes in each of these samples varies continuously over a certain range, so that there is no unique way to express their composite absorption bands using two representative pyroxene bands. In addition to those bands deconvolved in the Y980459 spectrum, there is a band around 1.05 μm (band 4) which may be assigned to Fe^{2+} in olivine.

The band center, full width at half maximum (FWHM), and scaled strength of Y980459 and these shergottite samples are plotted in Fig. 4. The relationship between the band center and FWHM is supposedly an indication of the nature of each absorption band. As seen in Fig. 4a, the bands 1a, 1b, and 3 of Y980459 have similar band center and width values to those of the shergottite samples. On the other hand, the bands

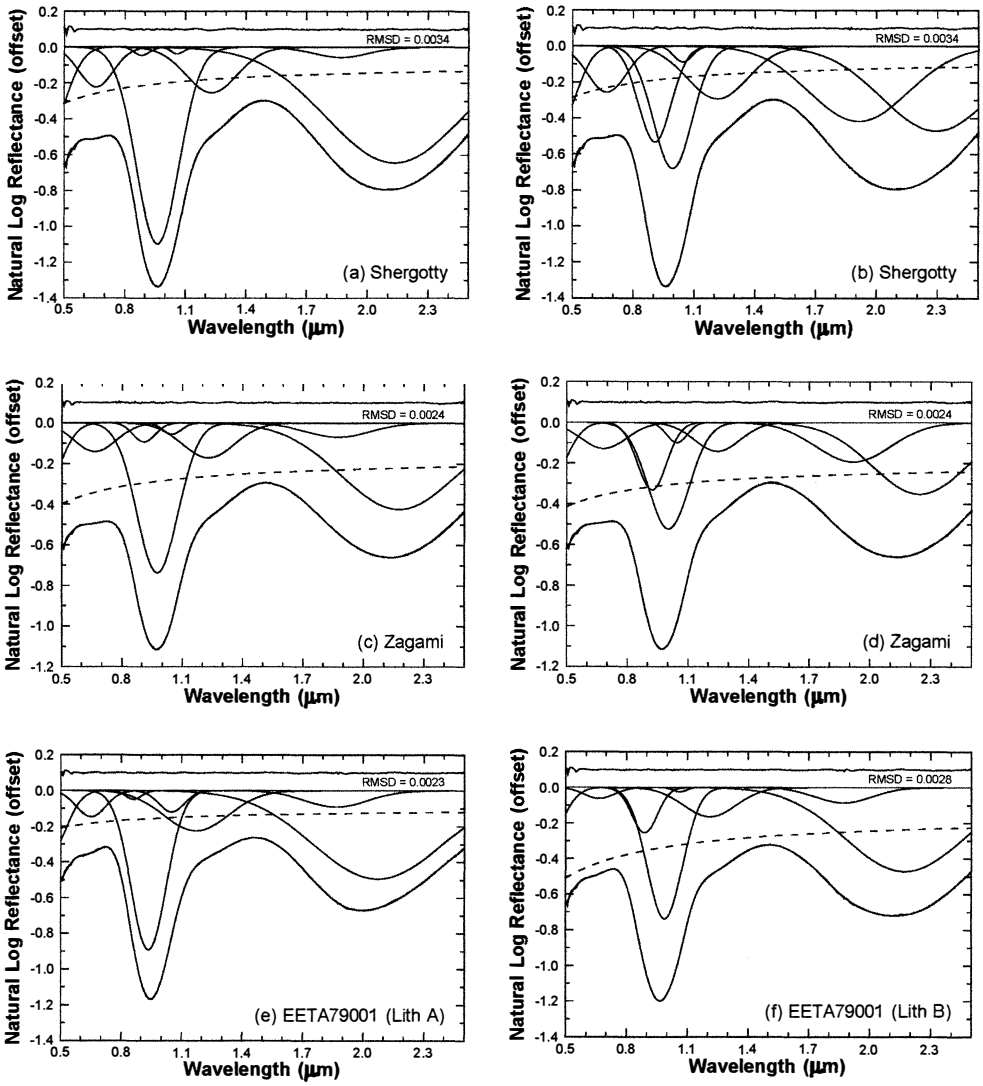

Fig. 3. Modified Gaussian model fits of the reflectance spectra of some shergottite powder samples (Sunshine et al., 1993; McFadden and Cline, 2004). Listed near the upper-right corner of each plot is the root mean square deviation (RMSD) of each fit.

2a and 2b of Y980459 are located to the short-wavelength side of the shergottite ranges. Because the bands 2a and 2b are assigned solely to pyroxenes and band center wavelengths of pyroxenes are correlated to their Ca and Fe contents (*e.g.*, Adams and McCord, 1972; Adams, 1974; Cloutis, 1985; Cloutis and Gaffey, 1991), these results suggest that low-Ca pyroxene in Y980459 has lower in Fe and/or Ca content than those in the shergottite samples, high-Ca pyroxene has similar Fe and Ca contents to those of EETA79001 (Lithology A) which are lower than those in other shergottite samples, and

Table 2. Optimized parameters for modified Gaussian model fits of reflectance spectra of other shergottites.

Band No.	Center (μm)	FWHM (μm)	Strength	Center (μm)	FWHM (μm)	Strength
		Shergotty			Shergotty	
1a	0.884	0.087	−0.045	0.907	0.189	−0.533
1b	0.962	0.248	−1.098	0.994	0.226	−0.680
2a	1.870	0.316	−0.055	1.913	0.576	−0.417
2b	2.134	0.790	−0.645	2.292	0.627	−0.471
3	1.230	0.300	−0.253	1.216	0.352	−0.293
4	1.060	0.073	−0.037	1.045	0.106	−0.088
		Zagami			Zagami	
1a	0.909	0.130	−0.093	0.921	0.169	−0.331
1b	0.975	0.240	−0.737	1.003	0.238	−0.523
2a	1.873	0.377	−0.068	1.917	0.433	−0.193
2b	2.175	0.674	−0.425	2.244	0.549	−0.351
3	1.229	0.305	−0.172	1.244	0.264	−0.142
4	1.048	0.109	−0.055	1.044	0.118	−0.098
		EETA79001 (Lith. A)			EETA79001 (Lith. B)	
1a	0.860	0.096	−0.048	0.889	0.146	−0.254
1b	0.936	0.205	−0.891	0.988	0.204	−0.738
2a	1.866	0.366	−0.091	1.871	0.324	−0.085
2b	2.072	0.755	−0.495	2.172	0.685	−0.471
3	1.170	0.380	−0.226	1.211	0.305	−0.165
4	1.049	0.149	−0.120	1.063	0.074	−0.024

the olivine phase made the bands 1a, 1b, and 3 have similar band centers and widths to the shergottite samples. The absence of band 4 in the Y980459 spectrum casts a shadow on the above interpretation of olivine and raises a question whether a mesostasis such as glass may have disturbed even the center wavelength values of the bands 2a and 2b. The above insight on the relationship of pyroxene composition between Y980459 and the shergottite samples is consistent with previous analyses of their pyroxene chemical compositions (*e.g.*, Mikouchi *et al.*, 1999).

Plotted in Fig. 4b are band center and scaled strength values. Band strengths of each sample are normalized by that of the band 1b which is stronger than any other bands plotted here. In this plot again, the bands 1a, 1b, and 3 of Y980459 fall in the same range with the shergottite samples, whereas its bands 2a and 2b show shorter center wavelengths and smaller relative strengths than those of the shergottite samples. This suggests that some other mineral phase (such as olivine and glass) than pyroxenes contributes to the band 1b strength of Y980459, making its bands 2a and 2b relatively weaker than the band 1b.

In order to characterize the mineral modal abundance of Y980459, spectra of several mixtures of olivine, pyroxene, and plagioclase (Hiroi and Pieters, 1994) shown in Fig. 5 have been deconvolved using the modified Gaussian model. The resulting band parameters are listed in Table 3 and plotted in Fig. 6 together with those for Y980459. As is seen in Fig. 6a, most of the Y980459 bands fall in the tricomponent mixture range except for the band 2a which has a much smaller band width than the mixtures. The relative band strengths plotted in Fig. 6b shows that the Y980459 bands

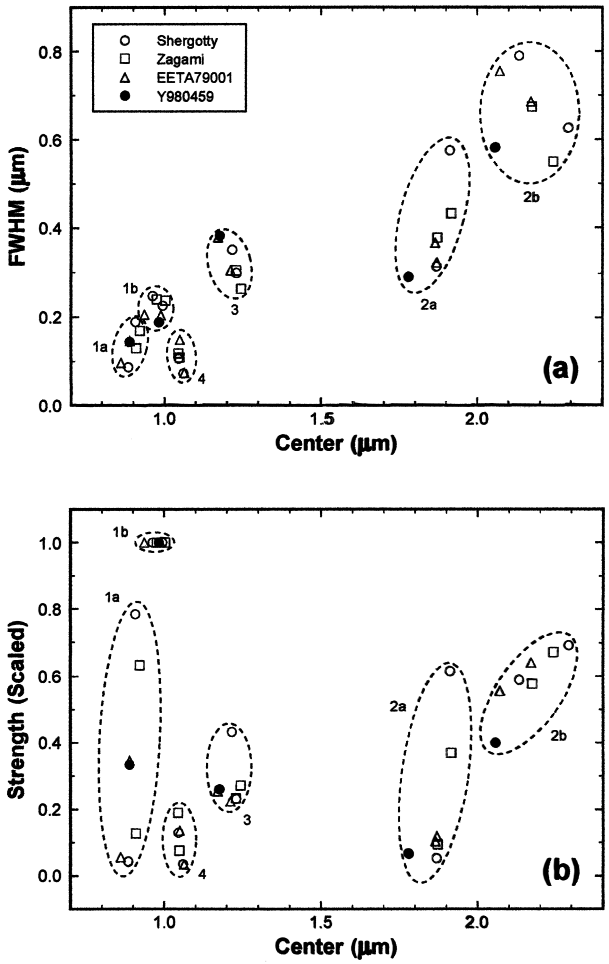

Fig. 4. Plots of optimized modified Gaussian parameters for the Y980459 and shergottite samples: (a) Band center vs. full width at half maximum (FWHM), and (b) Band center vs. strength normalized by the strength of Band 1b.

fall within the range of the tricomponent mixtures except for the band 1a. In all, none of the tricomponent mixtures matches with Y980459 in terms of the centers, widths, and relative strengths of all the bands. This suggests that a significant amount of other mineral components such as glass exist in Y980459 as one possibility.

Faced with this difficult situation of characterizing the mineral composition of Y980459 using the modified Gaussian model, we attempt to reduce these band parameter information to the old-fashioned scheme of the band II/band I area ratio for estimating the olivine/pyroxene ration (*e.g.*, Cloutis *et al.*, 1986). Using the formula for calculating the band area of each modified Gaussian:

$$(\text{Area}) = \sqrt{\pi/\ln 2}\,/2 \times |\,(\text{Strength})\,| \times (\text{FWHM}), \qquad (1)$$

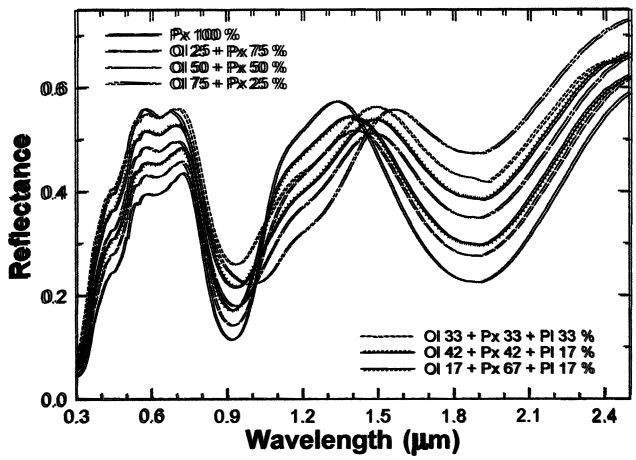

Fig. 5. Reflectance spectra of tricomponent mixtures of pyroxene (Px), olivine (Ol), and plagioclase (Pl) taken from the RELAB Database (Hiroi and Pieters, 1994). The grain size range of the minerals is 45–75 μm.

the band I area (sum of the band 1a, 1b, 3, and 4 areas), band II area (sum of the band 2a and 2b areas), and the band II/band I area ratio have been calculated for the shergottite samples and tricomponent mixtures as well as Y980459. The results are listed in Table 4.

After examining any correlation between the mixing ratios of the tricomponent mixtures and the band II/band I area ratios in Table 4, we found that the pyroxene abundance has the highest correlation as expected. This correlation is plotted in Fig. 7 together with the band II/band I area ratios of the shergottite samples and Y980459 using their mineral modal abundances taken from literature in Table 5. Figure 7 clearly depicts the uniqueness of Y980459 that it has much lower amount of pyroxene than the shergottite samples. The estimation of the pyroxene abundance using the band II/band I area ratio seems to be accurate within 13% of pyroxene abundance. If we were to estimate the pyroxene abundance of Y980459 without knowing any such analysis, we would give $36 \pm 13\%$ based on the trend in Fig. 7. This range includes the value of 48% estimated by an independent petrographical study (Mikouchi *et al.*, 2003, 2004).

On the other hand, there is a traditionally-established scheme of estimating the olivine and pyroxene modal abundance ratios (*e.g.*, Cloutis *et al.*, 1986; Burbine *et al.*, 2003). Linear continuum is removed as a tangential line for each of the bands I and II of reflectance spectrum, and the ratio of those two areas below the continuum lines is calculated. Cloutis *et al.* (1986) and Burbine *et al.* (2003) adopt different formula for converting the band area ratio (BAR) into the olivine/pyroxene ratio:

$$\text{Olivine}/(\text{Olivine}+\text{Pyroxene}) = -0.417\text{BAR} + 0.948 \quad (\text{Cloutis}), \tag{2}$$

$$\text{Olivine}/(\text{Olivine}+\text{Pyroxene}) = -0.228\text{BAR} + 0.768 \quad (\text{Burbine}). \tag{3}$$

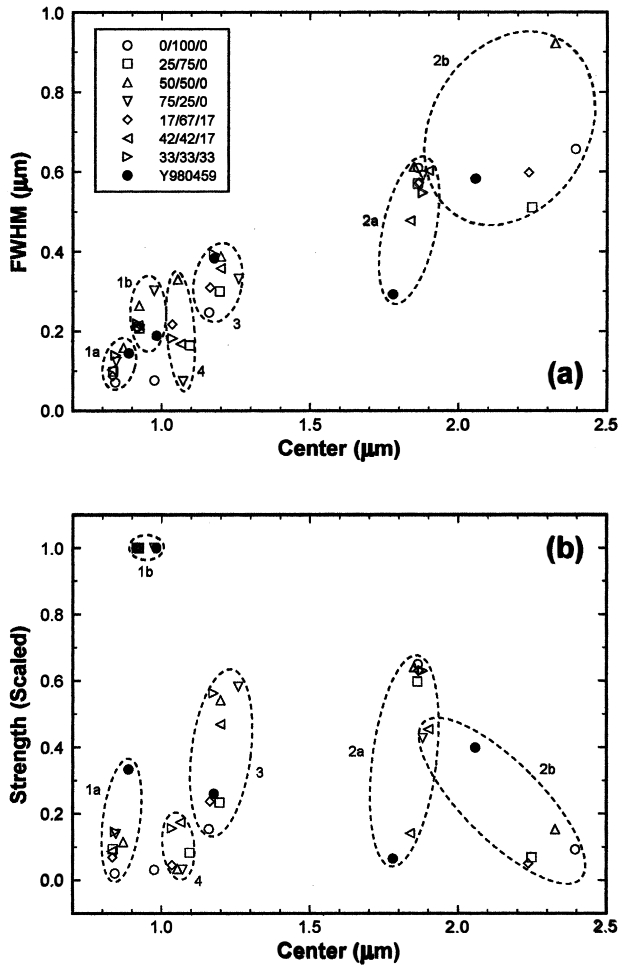

Fig. 6. Plots of optimized modified Gaussian parameters for the Y980459 sample and tricomponent mixtures: (a) Band center vs. full width at half maximum (FWHM), and (b) Band center vs. strength normalized by the strength of Band 1b.

The BAR of the reflectance spectrum of the Y980459 sample is 0.957, which gives 0.55 as the olivine/(olivine+pyroxene) ratio by either of the above formula, which then gives 0.45 as the pyroxene/(olivine+pyroxene) ratio. Although this 45% is close to the petrographically-derived value of 48% (Mikouchi *et al*., 2003, 2004), presence of a significant amount of mesostasis (25%) casts a shadow on the interpretation of the result. Strictly speaking, because the above reference gives 26% as olivine abundance, the pyroxene/(olivine+pyroxene) ratio becomes 0.65, which is not so close to 0.45 derived from eqs. (2) or (3). If we assume the mesostasis phase mostly contributes to the band I, estimating the pyroxene modal abundance using eqs. (2) or (3) can be justified, and the close match between their result of 45% and the petrographically-derived 48% makes sense. This match may be mainly due to the fact that Y980459

Table 3. Optimized parameters for modified Gaussian model fits of reflectance spectra of tricomponent mixtures of olivine, pyroxene, and plagioclase.

Band No.	Center (μm)	FWHM (μm)	Strength	Center (μm)	FWHM (μm)	Strength
	Olv 25%+Pyx 75%			Olv 17%+Pyx 67%+Plg 17%		
1a	0.835	0.098	−0.134	0.834	0.087	−0.084
1b	0.924	0.207	−1.439	0.917	0.207	−1.228
4	1.095	0.165	−0.119	1.036	0.217	−0.056
3	1.196	0.300	−0.336	1.163	0.310	−0.291
2a	1.863	0.572	−0.860	1.867	0.573	−0.774
2b	2.248	0.510	−0.098	2.237	0.598	−0.061
	Olv 50%+Pyx 50%			Olv 42%+Pyx 42%+Plg 17%		
1a	0.870	0.158	−0.132	0.832	0.103	−0.084
1b	0.924	0.264	−1.153	0.919	0.215	−0.969
4	1.054	0.330	−0.039	1.064	0.168	−0.169
3	1.199	0.388	−0.624	1.198	0.358	−0.454
2a	1.851	0.612	−0.739	1.838	0.476	−0.137
2b	2.327	0.922	−0.176	1.900	0.602	−0.440
	Olv 75%+Pyx 25%			Olv 33%+Pyx 33%+Plg 33%		
1a	0.846	0.123	−0.141	0.843	0.139	−0.107
1b	0.974	0.301	−1.010	0.916	0.219	−0.736
4	1.071	0.075	−0.032	1.036	0.183	−0.115
3	1.259	0.331	−0.588	1.175	0.394	−0.414
2a	1.881	0.591	−0.431	1.880	0.549	−0.464
	Pyx 100%					
1a	0.842	0.071	−0.036			
1b	0.915	0.212	−1.748			
1c	0.975	0.076	−0.055			
3	1.160	0.247	−0.269			
2a	1.864	0.609	−1.136			
2b	2.395	0.657	−0.161			

Table 4. Consolidated Band I and II areas and their ratios calculated from the optimized modified Gaussian model parameters of shergottite samples and tricomponent mixtures in Tables 1, 2, and 3.

Sample	Band I (1a+1b+3+4)	Band II (2a+2b)	Band II/I
Shergotty	0.384	0.565	1.459
Zagami	0.254	0.313	1.205
EETA79001	0.283	0.403	1.462
Y980459	0.155	0.116	0.747
Pyx 100%	0.473	0.849	1.794
Olv 25%+Pyx 75%	0.459	0.576	1.255
Olv 50%+Pyx 50%	0.618	0.654	1.060
Olv 75%+Pyx 25%	0.552	0.271	0.492
Olv 17%+Pyx 67%+Plg 17%	0.387	0.511	1.321
Olv 42%+Pyx 42%+Plg 17%	0.434	0.351	0.810
Olv 33%+Pyx 33%+Plg 33%	0.383	0.271	0.707

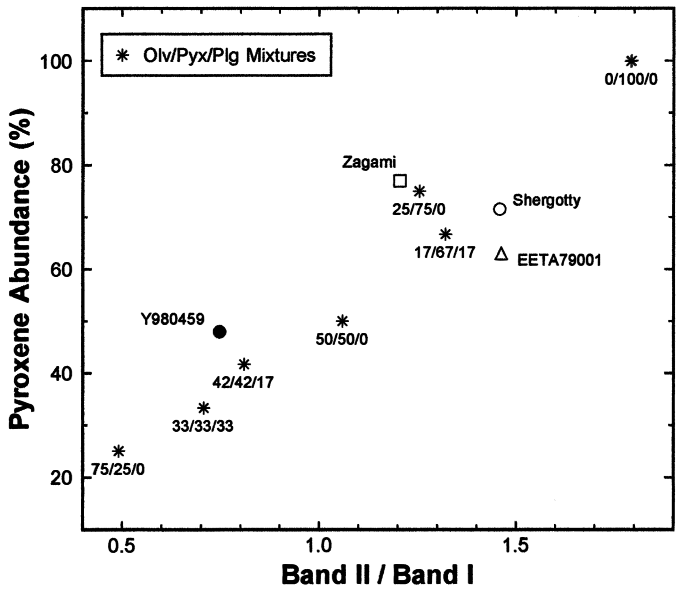

Fig. 7. A plot of Band II/Band I area ratio vs. pyroxene abundance of the Y980459 and shergottite samples, and tricomponent mixtures. Tricomponent points are shown as stars, and shergottite points as the same symbols as in Fig. 4. Shown next to each tricomponent mixture point is its mineral mixing ratio (%).

Table 5. Mineral modal abundances of shergottites in this study.

	Shergotty[*1]	Zagami[*2]	EETA79001[*3]	Y980459[*4]
Olivine	0.3		3	26
Pyroxenes	71.5	77	63	48
Plagioclase/maskelynite	23	15	22	
Mesostasis	1.2	3.4		25

[*1] Smith and Hervig (1979), [*2] McCoy *et al*. (1992), [*3] Schwandt *et al*. (2001), [*4] Mikouchi *et al*. (2003).

does not have any plagioclase (Mikouchi *et al*., 2003, 2004) which contributes to the band I but with much weaker optical activity than pyroxene or olivine.

4. Conclusions

1) Visible and near-infrared reflectance spectrum of our Y980459 sample is clearly different from the shergottite samples studied in this paper (Shergotty, Zagami, and EETA79001) in that it is darker, and has shallower absorption bands and a smaller band II/band I ratio.

2) Modified Gaussian model deconvolutions of the Y980459 sample, the shergottite samples, and tricomponent mixtures of olivine, pyroxene, and plagioclase suggest

that Y980459 has pyroxene phases which are lower in Fe and/or Ca than in the shergottites in our study except its high-Ca pyroxene having similar Fe and Ca contents to those in EETA79001 (Lithology A), and is richer in glassy phase than the shergottites.

3) Based on a correlation between the band II/band I area ratio and pyroxene abundance in the tricomponent mixtures and shergottite samples, the pyroxene abundance in Y980459 is estimated to be 36±13%, which overlaps with petrographically-derived value of 48%. Traditional scheme of estimating the band areas by removing linear tangential continuum gives a value of 45% under certain assumptions.

Acknowledgments

The authors appreciate the National Institute of Polar Research for providing them with a Yamato 980459 sample. Measurements of the shergottite spectra used in this study were initiated by Dr. Lucy A. McFadden using the RELAB facility. RELAB is a multiuser facility which is supported by NASA grant NAG5-13609 and is located at Brown University. TH thanks Dr. Carle Pieters for her support in writing this paper. Constructive reviews by Drs. Sho Sasaki and Tom Burbine contributed to a significant improvement of the manuscript.

References

Adams, J.B. (1974): Visible and near-infrared diffuse reflectance spectra of pyroxenes as applied to remote sensing of solid objects in the solar system. J. Geophys. Res., **79**, 4829–4836.

Adams, J.B. and McCord, T.B. (1972): Electronic spectra of pyroxenes and interpretation of telescopic spectral reflectivity curves of the moon. Proc. Lunar Sci. Conf., **3rd**, 3021–3034.

Burbine, T.H., McCoy, T.J., Jarosewich, E. and Sunshine, J.M. (2003): Deriving asteroid mineralogies from reflectance spectra: Implications for the MUSES-C target asteroid. Antarct. Meteorite Res., **16**, 185–195.

Cloutis, E.A. (1985): Interpretive techniques for reflectance spectra of mafic silicates. M. Sci. thesis, Univ. of Hawaii, Honolulu.

Cloutis, E.A. and Gaffey, M.J. (1991): Pyroxene spectroscopy revisited: Spectral-compositional correlations and relationship to geothermometry. J. Geophys. Res., **96**, 22809–22826.

Cloutis, E.A., Gaffey, M.J., Jakowski, T.L. and Reed, K.L. (1986): Calibrations of phase abundance, composition, and particle size distribution for olivine-orthopyroxene mixtures from reflectance spectra. J. Geophys. Res., **91**, 11641–11653.

Greshake, A., Fritz, J. and Stöffler, D. (2003): Petrography and shock metamorphism of the unique shergottite Yamato 980459. International Symposium—Evolution of Solar System Materials: A New Perspective from Antarctic Meteorites. Tokyo, Natl. Inst. Polar Res., 29–30.

Hiroi, T. and Pieters, C.M. (1994): Estimation of grain sizes and mixing ratios of fine powder mixtures of common geologic minerals. J. Geophys. Res., **99**, 10867–10879.

Ikeda, Y. (2003): Petrology of the Yamato 980459 shergottite. International Symposium—Evolution of Solar System Materials: A New Perspective from Antarctic Meteorites. Tokyo, Natl. Inst. Polar Res., 42.

Kojima, H. and Imae, N. (2002): Y980459. Meteorite Newslett., **11** (1), 48.

McCoy, T.J., Taylor, G.J. and Keil, K. (1992): Zagami: Product of a two-stage magmatic history. Geochim. Cosmochim. Acta, **56**, 3571–3582.

McFadden, L.A. and Cline, T.P. (2004): Spectral reflectance of martian meteorites: Spectral signatures as a template for locating source region on Mars. Meteorit. Planet. Sci. (in press).

Mikouchi, T., Miyamoto, M. and McKay, G. (1999): The role of undercooling in producing igneous zoning

trends in pyroxenes and maskelynites among basaltic Martian meteorites. Earth. Planet. Sci. Lett., **173**, 235–256.

Mikouchi, T., Koizumi, E., McKay, G., Monkawa, A., Ueda, Y. and Miyamoto, M. (2003): Mineralogy and petrology of the Yamato 980459 martian meteorite: A new shergottite-related rock. International Symposium—Evolution of Solar System Materials: A New Perspective from Antarctic Meteorites. Tokyo, Natl. Inst. Polar Res., 82–83.

Mikouchi1, T., Koizumi, E., McKay, G., Monkawa, A., Ueda, Y., Chokai, J. and Miyamoto, M. (2004): Yamato 980459: Mineralogy and petrology of a new shergottite-related rock from Antarctica. Antarct. Meteorite Res., **17**, 13–34.

Misawa, K. (2003): The Yamato 980459 shergottite consortium. International Symposium—Evolution of Solar System Materials: A New Perspective from Antarctic Meteorites. Tokyo, Natl. Inst. Polar Res., 84–85.

Pieters, C.M. (1983): Strength of mineral absorption features in the transmitted component of near-infrared reflected light—First results from RELAB. J. Geophys. Res., **88**, 9534–9544.

Schwandt, C.S., Jones, J.H., Mittlefehldt, D.W. and Treiman, A.H. (2001): The magma composition of EET 79001A: The first recount. Lunar and Planetary Science XXXII. Houston, Lunar Planet. Inst., Abstract #1913 (CD-ROM).

Smith, J.V. and Hervig, R.L. (1979): Shergotty meteorite: Mineralogy, petrography, and minor elements. Meteoritics, **14**, 121–142.

Sunshine, J.M., Pieters, C.M. and Pratt, S.F. (1990): Deconvolution of mineral absorption bands: An improved approach. J. Geophys. Res., **95**, 6955–6966.

Sunshine, J.M., McFadden, L.A. and Pieters, C.M. (1993): Reflectance spectra of the Elephant Moraine A 79001 meteorite: Implications for remote sensing of planetary bodies. Icarus, **105**, 79–91.